Hierarchical zeolite catalysed fructose dehydration to 5-hydroxymethylfurfural within a biphasic solvent system under microwave irradiation

Huaizhong Xiang[1], Shima Zainal[1], Henry Jones[2], Xiaoxia Ou[1,3], Carmine D'Agostino[1,4], Jesús Esteban[1,*], Christopher M. A. Parlett[1, 5, 6, 7*], and Xiaolei Fan[1,3*]

[1] *Department of Chemical Engineering, School of Engineering, The University of Manchester, Oxford Road, Manchester, M13 9PL, United Kingdom*
[2] *Department of Chemistry, The University of Manchester, Oxford Road, Manchester, M13 9PL, United Kingdom*
[3] *Nottingham Ningbo China Beacons of Excellence Research and Innovation Institute, University of Nottingham Ningbo China, 211 Xingguang Road, Ningbo 315100, China*
[4] *Dipartimento di Ingegneria Civile, Chimica, Ambientale e dei Materiali (DICAM), Alma Mater Studiorum – Università di Bologna, Via Terracini, 28, 40131 Bologna, Italy*
[5] *University of Manchester at Harwell, Diamond Light Source, Harwell Science and Innovation Campus, Didcot, Oxfordshire, OX11 0DE, United Kingdom*
[6] *Diamond Light Source, Harwell Science and Innovation Campus, Didcot, Oxfordshire, OX11 0DE, United Kingdom*
[7] *UK Catalysis Hub, Research Complex at Harwell, Rutherford Appleton Laboratory, Harwell, Oxfordshire, OX11 0FA, United Kingdom*

Electronic Supplementary Information (ESI)

Determination of catalytic performance

For catalytic fructose dehydration, the conversion of fructose (mol%), the product yield (mol%), product selectivity (%), and partition ratio of HMF (PR) were defined by Eqs. (S1)–(S4). Total energy efficiency coefficient (η) of the reaction was calculated according to Eq. (S5)

$$\text{Fructose conversion (mol\%)} = \frac{[Fru]_0 - [Fru]_t}{[Fru]_0} \times 100\ \% \quad \text{(S1)}$$

$$\text{Product yield (mol\%)} = \frac{[i]_t n_{ci}}{[Fru]_0 n_{Cfru}} \times 100\ \% \quad \text{(S2)}$$

$$\text{Product selectivity (\%)} = \frac{[i]_t n_{ci}}{([Fru]_0 - [Fru]_t) n_{Cfru}} \quad \text{(S3)}$$

$$\text{PR} = \frac{Mass\ fraction\ of\ HMF\ in\ the\ extraction\ phase}{Mass\ fraction\ of\ HMF\ in\ the\ reaction\ phase} \quad \text{(S4)}$$

$$\eta = \frac{[HMF]}{P \times t \times V} umol\ kJ^{-1}\ L^{-1} \quad \text{(S5)}$$

* Corresponding authors' emails: jesus.estebanserrano@manchester.ac.uk (J.E.S.); christopher.parlett@manchester.ac.uk (C.M.A.P.); xiaolei.fan@manchester.ac.uk (X.F.)

where *i* denotes the final products, i.e., fructose, glucose, HMF, levulinic acid, and formic acid; n_{ci} is the number of carbon atoms in species *i*; *Fru* denotes fructose; subscript *t* is the reaction time; subscript 0 denotes initial time (i.e., $t = 0$), and terms in brackets are concentrations in mol/L.

[HMF] is the amount of HMF produced (μmol); *P* is the consumed power by the reaction system (kW), *t* is the reaction time (s), and *V* is the reaction volume (L).

Green metrics calculations

Green chemistry metrics calculations (Eqs. (S6)–(S10))[1] were used to study the environmental impact and sustainability of the chemical reaction, with two E factors calculated. Both assume 100% product recovery and catalyst recyclability but differ regarding solvent recyclability. E factor (solvent recycled) assumes that the solvent is recycled, whereas E factor (solvent not recycled) assumes the solvent is not recycled.

E-factor (solvent recycled) = [Total mass of waste (excluding solvent)] / [Mass of final product] (S6)

E factor (solvent not recycled) = [Total mass of waste (including solvent)] / [Mass of final product] (S7)

MI = [Total mass in process] / [Mass of product] (S8)

RME (%) = [Mass of product] / [Total mass of reactants] × 100 (S9)

CE (%) = [Carbon in product] / [Total carbon in reactant] × 100 (S10)

where Mass of waste = Total mass of reactant – Total mass of product

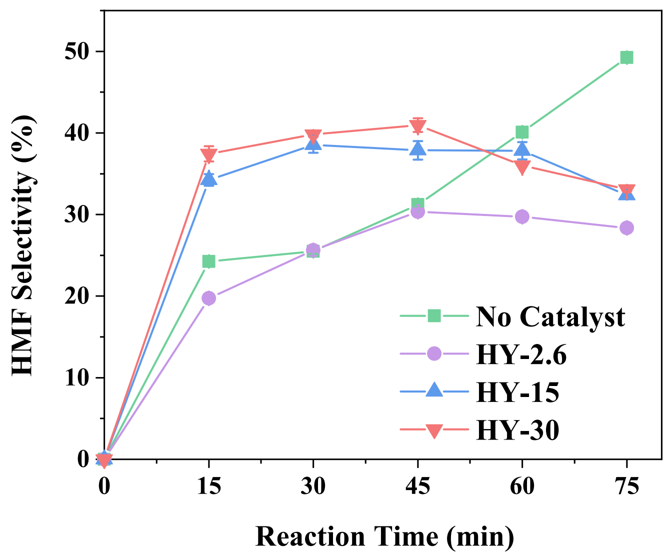

Fig. S1. HMF selectivity (as a function of the reaction time) for fructose dehydration in different aqueous systems under MW irradiation. Reaction conditions: 16 cm^3 water, 5 wt.% fructose, 2 wt.% zeolites, at 160 °C and 800 rpm.

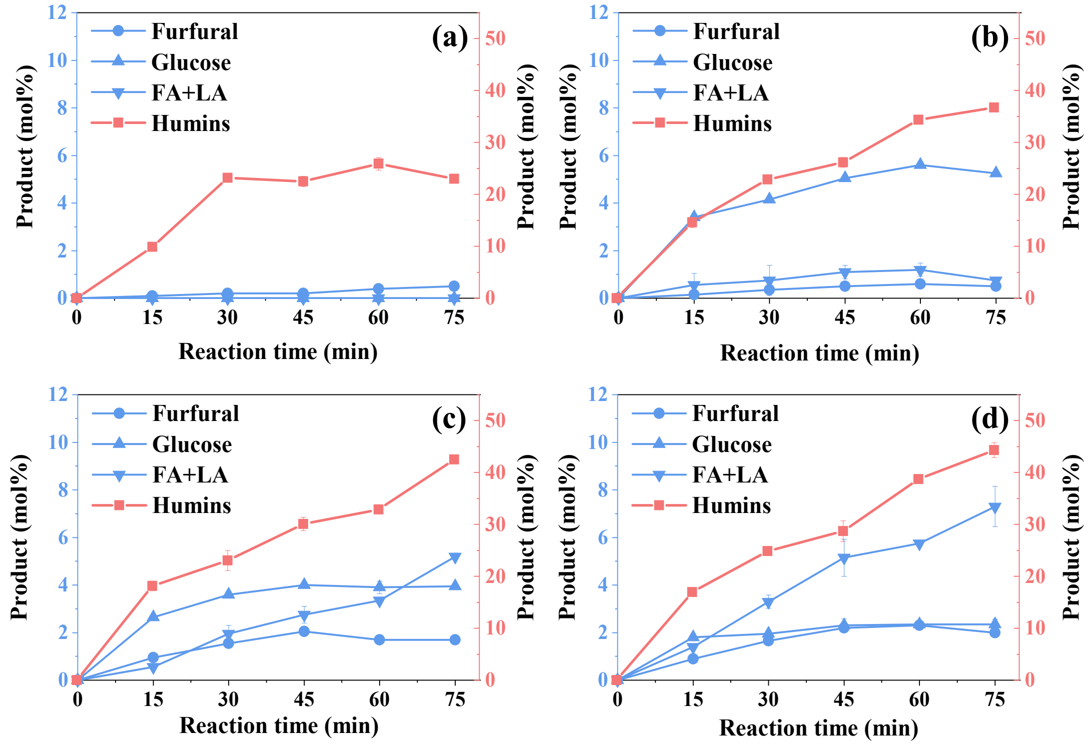

Fig. S2. By-product yield profiles for fructose dehydration in (a) catalyst-free system, and heterogeneous catalytic systems over (b) HY-2.6, (c) HY-15 and (d) HY-30 zeolites under MW irradiation. Reaction conditions: 16 cm^3 water, 5 wt.% fructose, 2 wt.% zeolites, at 160 °C and 800 rpm.

Turn over number (TON) and Turn over frequency (TOF)

$$\text{Turnover number (TON)} = \frac{Moles\ of\ HMF\ formed}{Number\ of\ active\ sites} \quad \text{(S11)}$$

$$\text{Turnover frequency (TOF)} = \frac{TON}{Time\ of\ reaction} \quad \text{(S12)}$$

Table S1. Dehydration of fructose into HMF over different zeolites in water.

Entry	Catalyst	Si/Ai ratio	Temp (℃)	Time (min)	Conversion (mol%)	Selectivity (%)	TOF (min^{-1})	Heating Method	Reference
1	H-Y	30	130	480	55.0	8.0	0.29	Autoclave	[2]
2	HZSM-5	25	130	480	52.0	13.0	0.11	Autoclave	[2]
3	H-BEA	12.5	130	480	74.0	8.5	0.02	Autoclave	[2]
4	H-Y	2.6	160	20	29.2	21.9	0.05	MW heating	[3]
5	HZSM-5	11.5	160	20	38.8	17.0	0.25	MW heating	[3]
6	H-BEA	12.5	160	20	76.6	21.0	0.33	MW heating	[3]
7	This Work	2.6	160	45	47.1	30.4	0.05	MW heating	/
8	This Work	15	160	45	62.6	37.9	0.46	MW heating	/
9	This Work	30	130	45	10.7	41.3	1.04	MW heating	/
10	This Work	30	160	45	65.0	41.0	6.32	MW heating	/

Table S2. Comparative study between conventional heating and MW heating for fructose dehydration over HY-30 zeolites in water.

Heating method	Fructose Conversion (mol%)	HMF Yield (μmol)	Consumed Power (kJ)	Energy efficiency (umol kJ^{-1} L^{-1})
Oil bath heating*	40.7	820	1152	59.9
Batch reactor	54.9	1260	806.4	89.4
MW heating	65.0	1180	381.6	168.1

Reaction conditions: 16 cm^3 water, 5 wt.% fructose, 2 wt.% HY-30 zeolites, at 160 ℃ and 800 rpm for 45 min. * reflux temperature.

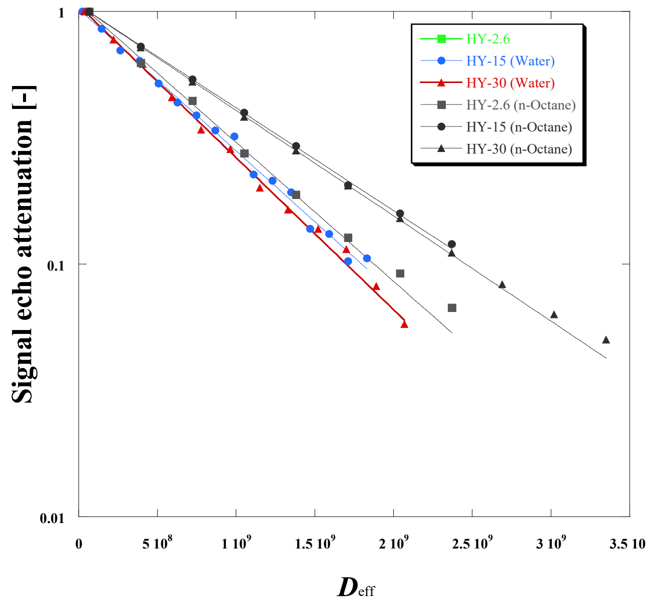

Fig. S3. PFG-NMR log attenuation plots for water and n-Octane within different HY-zeolites.

Table S3. Self-diffusion measurements of water within the HY-zeolites.

Catalysts	Self-Diffusion Coefficient of Bulk Liquid (10^{-9} $m^2\,s^{-1}$)	Self-Diffusion Coefficient within Zeolite (10^{-9} $m^2\,s^{-1}$)	PFG interaction parameter
	Water		
HY-2.6	2.52 ± 0.00	/	/
HY-15	2.52 ± 0.00	1.30 ± 0.01	1.97
HY-30	2.52 ± 0.00	1.36 ± 0.20	1.85
	***n*-Octane**		Tortuosity, $\tau = \frac{D_{bulk}}{D_{pore}}$
HY-2.6	2.46 ± 0.00	1.30 ± 0.04	1.95
HY-15	2.46 ± 0.00	0.94 ± 0.07	2.64
HY-30	2.46 ± 0.00	0.96 ± 0.05	2.57

The PFG interaction parameter is also reported. Values are compared with those of n-octane. The PFG interaction parameter of n-octane represents the tortuosity of the porous catalyst.

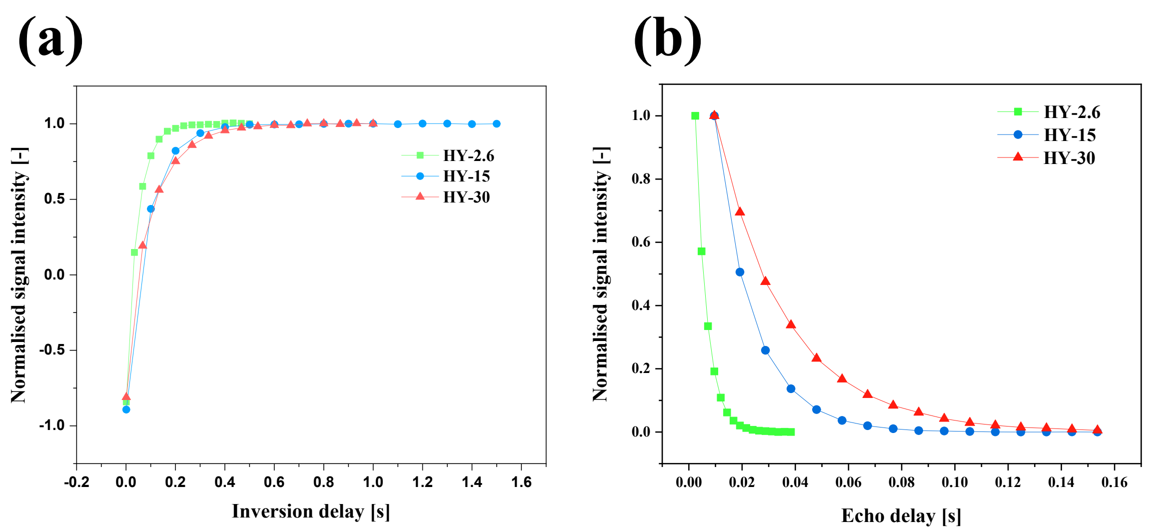

Fig. S4. Log attenuation plot of water imbibed in the HY zeolites under investigation.

Table S4. Values of T_1 and T_2 NMR relaxation time constants and their ratio T_1/T_2 for the three HY-zeolites in water and *n*-octane.

Catalysts	T_1[ms]	T_2 [ms]	T_1/T_2 [-]
		Water	
HY-2.6	44 ± 1.05	4.3 ± 0.66	10.2 ± 0.39
HY-15	83 ± 7.03	14 ± 1.86	5.82 ± 0.22
HY-30	94 ± 1.66	29 ± 1.16	1.30 ± 0.08
		***n*-octane**	
HY-2.6	1107 ± 0.00	628 ± 0.00	1.76 ± 0.11
HY-15	279 ± 33.0	198 ± 27.3	1.41 ± 0.02
HY-30	535 ± 01.65	278 ± 30.8	1.92 ± 0.03

Table S5. PR values for fructose dehydration to HMF in different biphasic reaction media.

Entry	Catalyst	Reactive phase (RP)	Extraction Phase (EP)	Volume ratio RP:EP	PR	Reference
1	Ion-exchange resin	Water	MIBK	1:1	1.36	4
2	Ion-exchange resin	Water:DMSO	MIBK	1:1	1.09	4
3	Ion-exchange resin	Water:DMSO	MIBK:2-BuOH	1:1	1.43	4
4	Diaion PK216	Water:DMSO	MIBK	1:1	0.74	5
5	HCl	Water:DMSO	MIBK:2-BuOH	1:2	1.10	6
6	HY-30	Water:DMSO	MIBK:2-BuOH	1:3	1.30	This work

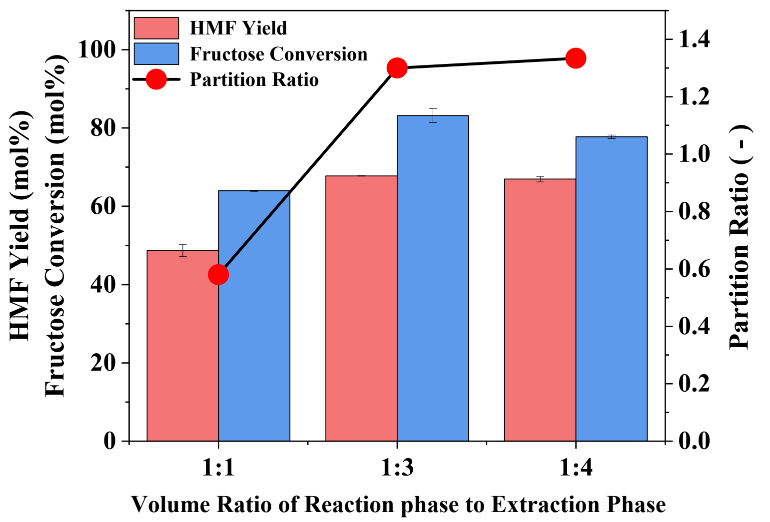

Fig. S5. Effect of volume ratio of Reaction phase to Extraction phase on fructose conversion, HMF yield and partition ratio. Reaction conditions: 16 cm^3 solvents, 5 wt.% fructose, 2 wt.% HY-30 zeolite, 6:4 (v/v) Water:DMSO / 7:3 (v/v) MIBK:2-BuOH (reaction phase:extraction phase (v:v) = 3), at 160 °C and 800 rpm for 45 min.

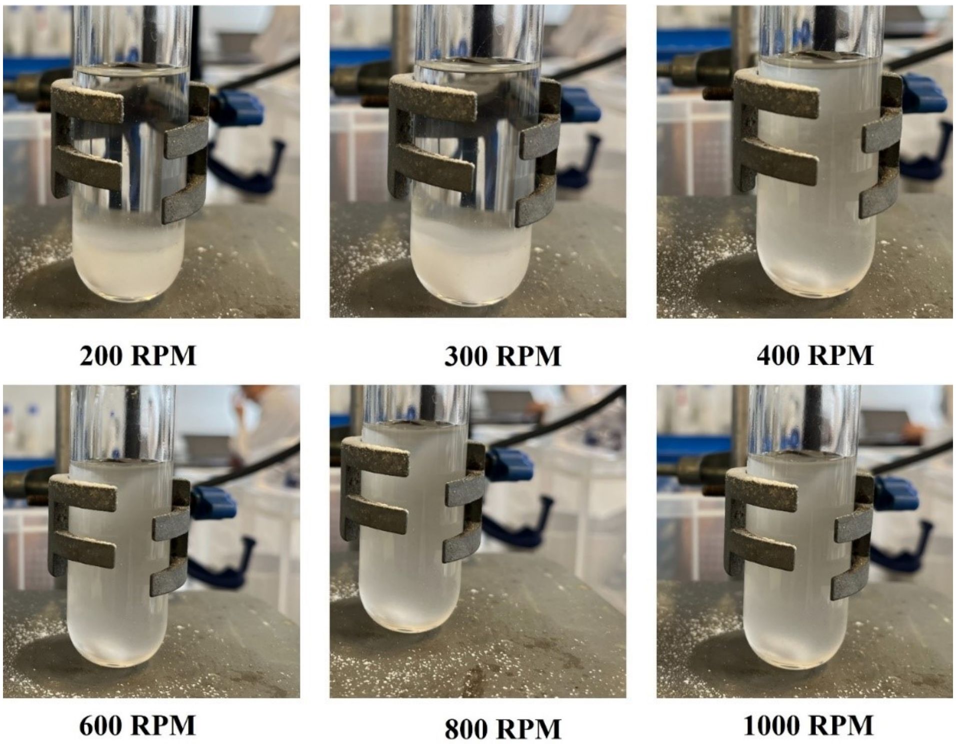

Fig. S6. Effect of stirring rate on mixing and catalyst distribution in a solvent system containing 6:4 (v/v) Water: DMSO / 7:3 (v/v) MIBK: 2-BuOH with reaction phase:extraction phase (v:v) = 3, total volume 16 cm^3.

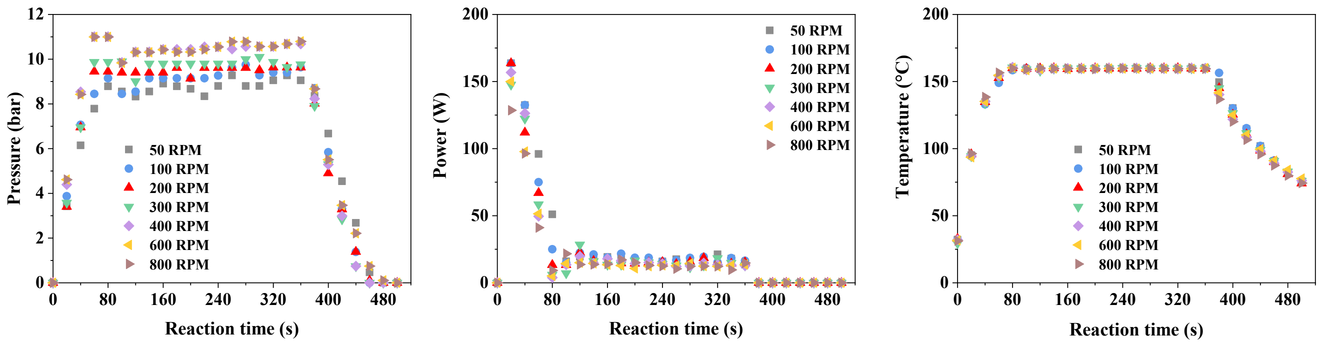

Fig. S7. Pressure, temperature, and power of the MW reactor during fructose dehydration over HY-30. Reaction conditions: 16 cm^3 solvents, 5 wt.% fructose, 2 wt.% HY-30 zeolite, 6:4 (v/v) Water:DMSO / 7:3 (v/v) MIBK:2-BuOH (reaction phase:extraction phase (v:v) = 3), at 160 °C and 800 rpm for 5 min.

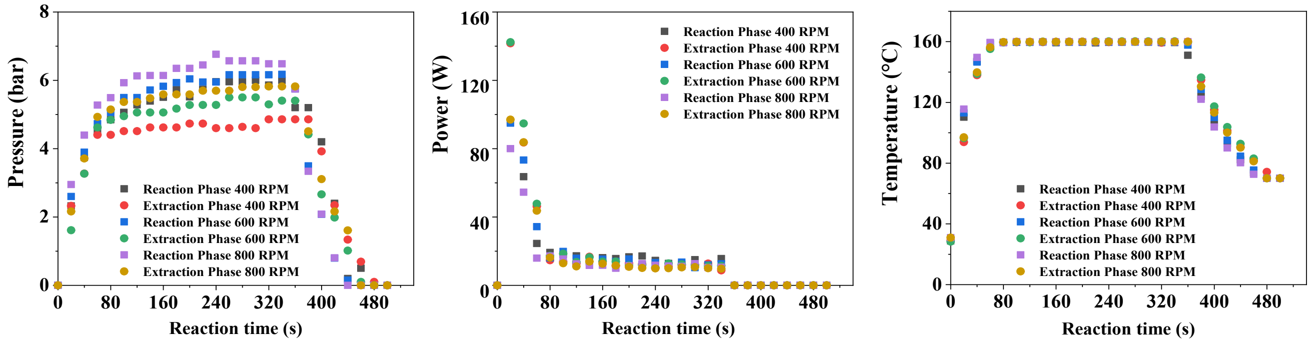

Fig. S8. Pressure, temperature, and power of the MW reactor during heating the reaction phase or extraction phases separately.

Table S6. Energy efficiency of HMF production at different reaction conditions for the optimal 6:4 (v/v) Water: DMSO / 7:3 (v/v) MIBK: 2-BuOH reaction media with a reaction phase:extraction phase (v:v) = 3 over the HY-30 zeolite. [a]

Reaction temperature (°C)	Reaction time (min)	HMF Yield (μmol)	Consumed Power (kJ)	Energy efficiency (μmol kJ^{-1} L^{-1})	E-factor (solvent recycled)
180	45	830.4	1116.0	46.5	0.91
160	45	820.4	439.2	116.7	0.93
140	240	702.7	1677.6	26.2	2.40

[a] Reaction conditions: 16 mL total reaction media volume, 5 wt.% fructose, 2 wt.% HY-30 at 200 rpm.

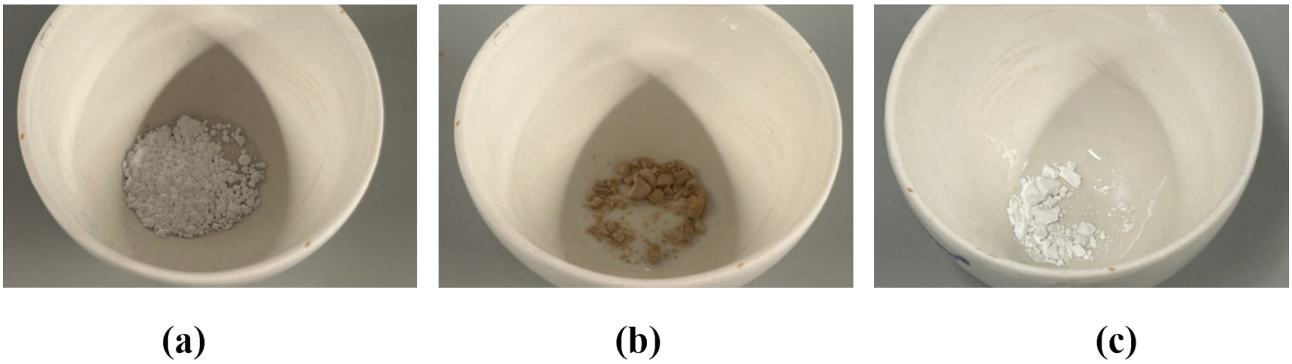

Fig. S9. Colour variations of catalyst from (a) before reaction; (b) after reaction; (c) used catalyst after calcination.

Table S7. Comparison of different heterogeneous catalysts for fructose dehydration to HMF using biphasic systems, ranked in reverse order of the selectivity to HMF.

Entry	Catalyst	Reactive phase	Extraction phase	Temp (°C)	Time (min)	Conversion (%)	Selectivity (%)	E (solvent recycled)	E (solvent not recycled)	MI	RME (%)	CE (%)	Ref.
1	SBA-15-PrSO_3H	Water	MIBK:2-BuOH	140	30	77.0	13.0	13.27	339.6	42.8	7.0	10.0	7
2	SiO_2/H-MOR	Water	MIBK	165	150	75.0	44.0	3.33	225.3	5.2	23.1	33.0	8
3	H-ZSM5	Water	MIBK	195	30	100.0	49.0	1.92	86.5	3.9	34.3	49.0	9
4	SBA-15-PrSH	Water	MIBK:2-BuOH	180	120	61.0	52.0	3.50	49.5	5.0	22.2	31.7	10
5	SBA-15	Water	MIBK:2-BuOH	180	120	59.0	52.0	3.66	51.2	5.2	21.5	30.7	10
6	Pyrochlores	Water	MIBK	150	120	99.0	59.6	1.42	141.3	4.0	41.3	59.0	11
7	Diaion PK216	Water: DMSO	MIBK	90	1260	68.0	60.0	2.50	73.5	38.5	28.6	40.8	5
8	Amberlyst 70	Water	MIBK:2-BuOH	130	225	85.0	60.0	1.80	30.8	3.0	35.7	51.0	12
9	H-MOR	Water	MIBK	165	300	60.0	60.0	2.97	206.5	4.8	25.2	36.0	8
10	Taa-A380	Water	MIBK:2-BuOH	180	120	62.0	61.0	2.78	41.6	4.2	26.5	37.8	10
11	SBA-15-PrSO3H	Water	MIBK:2-BuOH	140	30	78.0	62.0	1.95	70.5	8.9	33.9	48.4	7
12	Tp-A380	Water	MIBK:2-BuOH	180	120	67.0	64.0	2.33	36.6	3.7	30.0	42.9	10
13	SSA-SBA-15	Water	MIBK:2-BuOH	130	140	81.0	65.0	1.71	29.8	3.2	36.9	52.7	12
14	SBA-15-PrSO3H	Water	MIBK:2-BuOH	130	140	79.0	66.0	1.74	30.1	3.1	36.5	52.1	12
15	Amberlyst-70	Water	MIBK:2-BuOH	180	10	86.0	66.9	1.48	27.3	2.8	40.3	57.5	10
16	Resin catalyst	Water: DMSO	MIBK	90	90	74.0	68.0	1.84	59.6	5.7	35.2	50.3	4
17	TESAS-SBA-15	Water	MIBK:2-BuOH	130	140	84.0	71.0	1.40	26.3	3.2	41.7	59.6	12
18	HY-30 (this work)	Water: DMSO	MIBK:2-BuOH	140	240	88.8	71.3	1.26	157.9	3.2	44.3	63.3	/
19	SBA-15-PrSO3H	Water	MIBK:2-BuOH	180	120	66.0	74.0	1.93	32.2	3.3	34.2	48.8	10
20	HY-30 (this work)	Water: DMSO	MIBK:2-BuOH	180	45	99.5	75.2	0.91	133.6	2.7	52.4	74.8	/
20	Sulfonated MCM-41	Water	MIBK	190	45	98.0	78.6	0.85	18.2	1.9	53.9	77.0	13
21	PS-PP/C-foam-1	Water	MIBK	135	270	29.0	80.0	5.16	215.7	7.4	16.2	23.2	14
22	Heteropolyacids	Water	MIBK	170	160	88.7	80.3	1.00	49.3	2.2	49.9	71.3	15
23	H-MOR	Water	MIBK	165	90	87.0	85.0	0.93	98.6	2.5	51.8	74.0	16
24	HY-30 (this work)	Water: DMSO	MIBK:2-BuOH	160	45	85.9	86.1	0.93	135.3	2.7	51.7	73.9	/
25	SAPO-44	Water	MIBK	175	60	89.0	88.0	0.82	93.1	2.3	54.8	78.3	17
26	$Ag_3PW_{12}O_{40}$	Water	MIBK	120	60	82.9	93.8	0.84	19.0	1.9	54.4	77.7	18
27	$Cs_{2.5}H_{0.5}PW_{12}O_{40}$	Water	MIBK	115	60	78.2	94.7	0.93	23.8	2.3	51.8	74.0	19
28	HY-30 (this work)	Water: DMSO	MIBK:2-BuOH	140	120	42.5	98.8	2.40	238.0	4.8	29.4	42.0	/

References

1. R. A. Sheldon, *ACS Sustainable Chemistry & Engineering*, 2017, **6**, 32-48.
2. V. Rac, V. Rakić, D. Stošić, O. Otman and A. Auroux, *Microporous and Mesoporous Materials*, 2014, **194**, 126-134.
3. X. Jia, I. K. M. Yu, D. C. W. Tsang and A. C. K. Yip, *Microporous and Mesoporous Materials*, 2019, **284**, 43-52.
4. Y. Román-Leshkov, J. N. Chheda and J. A. Dumesic, *Science*, 2006, **312**, 1933-1937.
5. J. N. Chheda and J. A. Dumesic, *Catalysis Today*, 2007, **123**, 59-70.
6. J. N. Chheda, Y. Román-Leshkov and J. A. Dumesic, *Green Chemistry*, 2007, **9**, 342-350.
7. B. Karimi and H. M. Mirzaei, *RSC Advances*, 2013, **3**.
8. V. V. Ordomsky, J. van der Schaaf, J. C. Schouten and T. A. Nijhuis, *Journal of Catalysis*, 2012, **287**, 68-75.
9. M. Moreno-Recio, J. Santamaría-González and P. Maireles-Torres, *Chemical Engineering Journal*, 2016, **303**, 22-30.
10. A. J. Crisci, M. H. Tucker, J. A. Dumesic and S. L. Scott, *Topics in Catalysis*, 2010, **53**, 1185-1192.
11. S. F. Mayer, H. Falcón, R. Dipaola, P. Ribota, L. Moyano, S. Morales-delaRosa, R. Mariscal, J. M. Campos-Martín, J. A. Alonso and J. L. G. Fierro, *Molecular Catalysis*, 2020, **481**.
12. A. J. Crisci, M. H. Tucker, M.-Y. Lee, S. G. Jang, J. A. Dumesic and S. L. Scott, *ACS Catalysis*, 2011, **1**, 719-728.
13. Y. Huang, P.-Y. Chao, T.-Y. Cheng, Y. Ho, C.-T. Lin, H.-Y. Hsu, J.-J. Wong and T.-C. Tsai, *Chemical Engineering Journal*, 2016, **283**, 778-788.
14. V. V. Ordomsky, J. C. Schouten, J. van der Schaaf and T. A. Nijhuis, *Chemical Engineering Journal*, 2012, **207-208**, 218-225.
15. G. Lv, L. Deng, B. Lu, J. Li, X. Hou and Y. Yang, *Journal of Cleaner Production*, 2017, **142**, 2244-2251.
16. C. Moreau, R. Durand, S. Razigade, J. Duhamet, P. Faugeras, P. Rivalier, P. Ros and G. Avignon, *Applied Catalysis A: General*, 1996, **145**, 211-224.
17. P. Bhaumik and P. L. Dhepe, *RSC Advances*, 2013, **3**.
18. C. Fan, H. Guan, H. Zhang, J. Wang, S. Wang and X. Wang, *Biomass and Bioenergy*, 2011, **35**, 2659-2665.
19. Q. Zhao, L. Wang, S. Zhao, X. Wang and S. Wang, *Fuel*, 2011, **90**, 2289-2293.